

Influence of Contact-Line Curvature on the Evaporation of Nanodroplets from Solid Substrates

Jianguo Zhang,^{*} Frédéric Leroy, and Florian Müller-Plathe

*Eduard-Zintl-Institut für Anorganische und Physikalische Chemie and Center of Smart Interfaces,
Technische Universität Darmstadt, Alarich-Weiss-Straße 4, D-64287 Darmstadt, Germany*

(Received 20 January 2014; revised manuscript received 23 June 2014; published 21 July 2014)

The effect of the three-phase contact-line curvature on the evaporation mechanism of nanoscopic droplets from smooth and chemically homogenous substrates is studied by molecular dynamics simulations. Spherical droplets, whose three-phase contact line is curved, and cylindrical droplets, whose contact radius is infinite, are compared. It is found that the evaporation of cylindrical droplets takes place at constant contact angle, while spherical droplets evaporate by simultaneous reduction of their contact area and their contact angle. This is independent of the substrate-liquid interaction strength. The dependence of the evaporation mechanism on the contact-line curvature can be rationalized with the help of the concept of a contact-line tension, and the evaporation simulations of the spherical droplets are used to extract the line tension on each surface. The corresponding values for the Lennard-Jones systems studied here are of the order of 10^{-11} N, which is in a good agreement with previous theoretical and experimental estimates. With this order of magnitude, the line tension is expected to have an effect on the contact angle of spherical droplets only, when their diameter is less than about 100 nm. The observed difference in evaporation mechanism is interpreted as a manifestation of the line tension whose existence has been controversial.

DOI: [10.1103/PhysRevLett.113.046101](https://doi.org/10.1103/PhysRevLett.113.046101)

PACS numbers: 68.03.Fg

Increasing effort has been directed towards the numerous phenomena involving droplets on surfaces, such as wetting, spreading, condensation, and evaporation [1–12], for the past two decades. As one example, Furuta *et al.* [12] reported an experimental study of water droplets evaporating from both hydrophilic and hydrophobic substrates. Droplets with sizes about 0.1 and 1 mm were studied. The authors showed that both the nature of the substrate and the droplet size had an influence on the evaporation mechanism. This observation was interpreted as arising from the sign of the line tension, which varied depending on the nature of the coating.

Observations like this are evidence that the wetting behavior is not only determined by the balance of interfacial tensions, but also by the geometry of the adsorbed droplets and in particular the curvature of the three-phase contact line (TPCL). One rationalization uses the concept of a line tension, which refers to the excess free energy per unit length of the three-phase (gas-liquid-solid) contact line. It is expected to play a significant role at small droplet sizes, as the excess free energy of molecules in the vicinity of the TPCL is expected to be different from that in the bulk or at the interfaces [13] and the relative proportion of such molecules grows with decreasing droplet diameter. In practice, the line tension τ is often considered as a first-order correction of Young's equation and is defined by the so-called modified Young's equation

$$\gamma_{lv} \cos \theta_R = \gamma_{lv} \cos \theta_\infty - \frac{\tau}{R} = (\gamma_{sv} - \gamma_{sl}) - \frac{\tau}{R}, \quad (1)$$

where R is the contact-line radius (i.e., the inverse of its curvature), γ_{sv} , γ_{sl} , and γ_{lv} are the solid-vapor, solid-liquid,

and liquid-vapor interfacial tensions, respectively; θ_R and θ_∞ are the apparent contact angle of a droplet of contact-line radius R and the contact angle of a macroscopic droplet, respectively. From Eq. (1), it is clear that, for small enough droplets, the contact angle depends on the line tension and the contact-line curvature. Thus, depending on the sign of τ and the magnitude of the term τ/R relative to the surface tensions term $(\gamma_{sv} - \gamma_{sl})$, increasing-, decreasing-, or constant-contact-angle values are expected as an evaporating drop shrinks. However, despite considerable theoretical and experimental efforts, the line tension still remains controversial, not only in terms of its magnitude, but also its sign. David [13] stated that if only van der Waals interactions are acting at the solid-liquid interface, the line tension is of the order of 10^{-11} N. The line tension was experimentally reported with values ranging from 10^{-5} to 10^{-11} N and with both positive and negative signs [1,3,7,14,15]. Theoretically, values of the order of 10^{-10} – 10^{-12} N have been found [8,16]. The discrepancies arise because the line tension has a weak effect and is therefore hard to determine. This scatter of line-tension values over several orders of magnitude has cast doubts on its role in static and dynamic wetting processes. The disagreements have been attributed, for example, to weak substrate heterogeneities rather than the line tension [4]. Moreover, not only the role of line tension, but its very existence, has been questioned. For example, Ward and Wu [17] suggested that no contact-line curvature term is needed to supplement Young's equation because the adsorption and its effect on the solid-liquid interfacial

tension instead of the line tension can fully explain the dependence of the contact angle on the contact-line curvature. The conclusion of Ward and Wu was later questioned by Schimmele and Dietrich [18] who noted that the applicability of Eq. (1) is clearly supported by experiments even in a restricted range of length scales.

It is thus clear that no consensus has been reached regarding the role played by the line tension. Whether and on which kinds of substrates it is important and at which length scales its role becomes significant cannot be easily answered by experiments. First, it is not easy to prepare an ideal surface without heterogeneities. Second, it is not easy to produce and control droplets of submicrometer size where the line tension is expected to be significant. The lack of experimental information hampers the comparison with theoretical models and their validation. It is therefore difficult to decipher the behavior of an evaporating droplet while several effects of similar magnitude may operate simultaneously.

Molecular simulations have a great advantage in that they do not require a specific theoretical framework to isolate contributions from different causes. Moreover, surface heterogeneities can be fully controlled. Simulations can, therefore, test assumptions or obtain information directly, without resorting to assumptions. They also naturally address length scales below 100 nm where line tension is expected to play a role in systems dominated by van der Waals interactions. In the present work, we use molecular dynamics (MD) simulations to study the evaporation of nanometer-sized droplets with different shapes. Spherical and cylindrical droplets with curved and straight TPCLs, respectively, are compared to study the influence of contact-line curvature by varying $1/R$.

In a previous simulation [10], the evaporation of spherical nanodroplets (starting at about 10 nm in diameter) on a perfectly smooth and chemically homogeneous heated substrate has been investigated by MD simulations. We found that neither the pure evaporation mode where the contact

line remains pinned (constant-contact-line mode) nor the pure evaporation mode where the contact angle remains constant (constant-contact-angle mode) prevailed during the evaporation. Instead, we observed that both contact angle and contact line were simultaneously changing. The contribution of the line tension to these observations remained unclear. In the present contribution, we therefore study the evaporation of cylindrical droplets on an ideally smooth and chemically homogeneous substrate. By construction, the contact line is straight, corresponding to an infinite contact-line radius R . Hence, according to the modified Young's equation [Eq. (1)] the line-tension term τ/R cancels and any line tension effect vanishes. In order to perform a direct comparison, the cylindrical and spherical droplet systems were constructed with the same liquid and solid models, similar droplet size in spherical radius, and similar evaporation rate (controlled by the rate of removing particles from the gas phase).

The simulation setup for cylindrical and spherical droplets is shown in Fig. 1. Similarly to our previous simulation [10], both the droplet and the substrate consisted of Lennard-Jones atoms with the nonbonded 12-6 potential

$$U(r) = 4\epsilon \left[\left(\frac{\sigma}{r} \right)^{12} - \left(\frac{\sigma}{r} \right)^6 \right]. \quad (2)$$

The interaction parameters and the simulation parameters are reported in the Supplemental Material [19]. All quantities are presented in reduced units (and noted with an asterisk). Identical solid-fluid interaction parameters were employed for the cylindrical droplet and spherical droplet systems. The values of the energy parameter ϵ^* for the fluid-solid interactions were 0.4, 0.6, and 0.7. In reference to these values, the corresponding systems were denoted S4, S6, and S7 for spherical droplet systems, and C4, C6, and C7 for cylindrical systems.

The substrate temperature was set to $T^* = 0.83(100 \text{ K})$ for both the cylindrical and the spherical droplet systems.

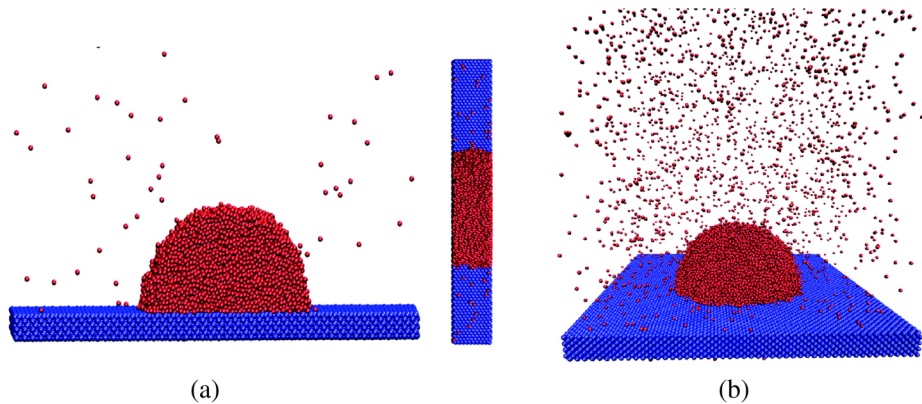


FIG. 1 (color online). (a) Cylindrical droplet on a substrate. The left picture is the front view; the right one is the top view. (b) Spherical droplet on a substrate.

After a period of relaxation, the droplets took their cylindrical or spherical shapes and were brought into thermal equilibrium with the substrates. A run of about $5000t^*$ (10 ns) was performed to ensure that the droplet and its vapor were in equilibrium. After equilibration at $T^* = 0.83$, a steady droplet was formed, the number of atoms inside the droplet was about 8000 for C4, C6, and C7, and about 14 000 for S4, S6, and S7. For all systems, the evaporation was subsequently driven by removing gas particles at a rate of 1 atom every 400 time steps (1.66×10^{-12} mol/s). The atom coordinates were recorded every 2000 time steps until the droplet completely disappeared. To study the effect of the TPCL curvature, both the contact angle and contact radius (half of the distance between the contact lines) were calculated (see details in Supplemental Material [19]). Note that due to the interaction between the solid and the liquid, a layer structure with an oscillating mass distribution is observed in the liquid near the liquid-solid interface (see Figs. S1, S2, and S3 in the Supplemental Material [19]). Such a behavior is commonly found in liquids near attractive walls [8,22,23,24]. It is worth mentioning that this structure is

a result of MD simulations rather than a model assumption. Therefore, the structure and any effects resulting from it are automatically allowed for in the simulation. The time evolution of the contact angle and contact radius for the spherical and the cylindrical droplet systems is shown in Fig. 2.

As can be seen in Figs. 2(a) and 2(b), both the contact angle and contact radius decrease simultaneously for the spherical droplet systems S4, S6, and S7, suggesting a mixed evaporation mode, which is the same as we have found in our previous simulation of a spherical droplet system [10]. This also indicates that the evaporation protocol of suddenly enlarging the box in our previous simulation and of removing gas atoms one by one does not lead to different evaporation modes. For the cylindrical droplets [Figs. 2(c) and 2(d)], however, all contact angles remain constant and the pseudocontact radius decreases continuously during the evaporation until the droplets become too small [contact radii less than 6σ (about 2 nm) for systems C4 and S4 and less than about 10σ (about 3 nm) for the others] to calculate unambiguously their contact angle. The equilibrium contact angles of systems C4, C6, and C7 are $115.0^\circ \pm 6.9^\circ$, $83.5^\circ \pm 3.5^\circ$, and $68.7^\circ \pm 4.2^\circ$, respectively, at a temperature $T^* = 0.83$.

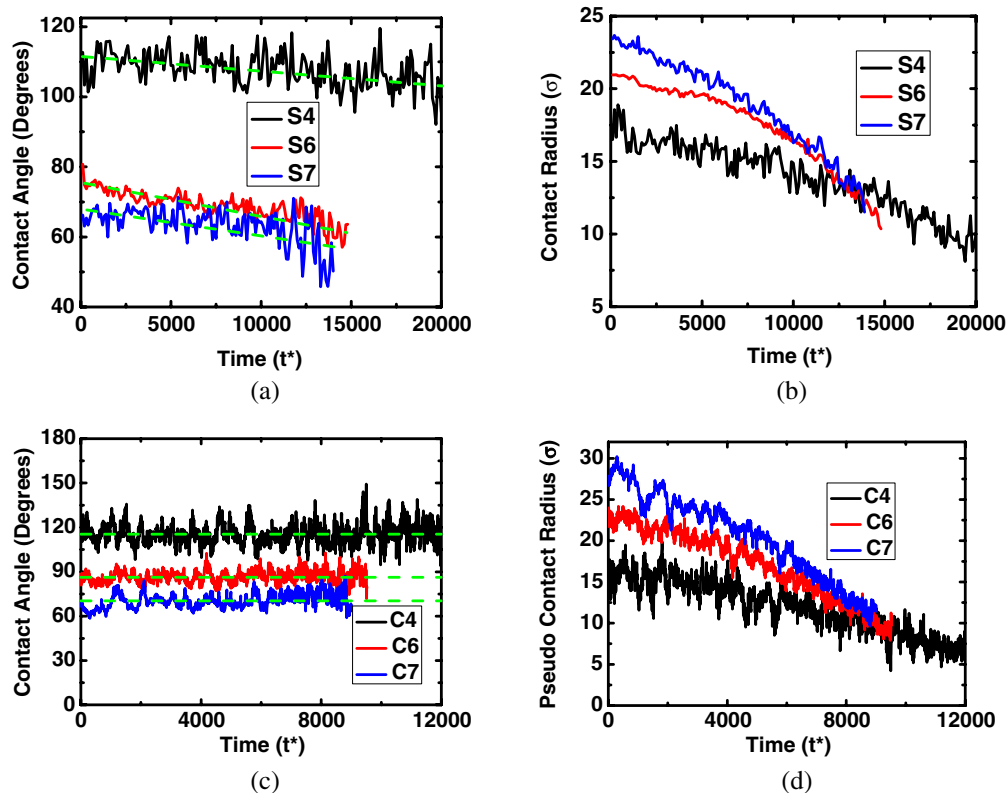


FIG. 2 (color online). Droplet evaporation at $T^* = 0.83$: time evolution of the spherical droplets' (a) contact angles and (b) contact radii; time evolution of the cylindrical droplets' (c) contact angles and (d) pseudocontact radii defined as half the distance between two contact lines. The dashed lines are the linear least-squares fits to the contact angle and show its decreasing behavior in (a) and indicate its average value in (c).

Evidently, the evaporation of the cylindrical droplet follows a pure constant-contact-angle evaporation mode. The mechanism contrasts with the mixed mode of the spherical droplets. Experimentally, a constant-contact-angle mode is often observed for spherical droplets of much larger size (small contact-line curvature), e.g., with a diameter $>1 \mu\text{m}$ [11,12].

The spherical and the cylindrical droplets have similar sizes (similar radius of the cap), they are subjected to similar evaporation rates (removing one atom every 400 time steps), and they are deposited on a substrate with the same wetting properties. They only differ in their contact-line curvatures. Thus, the contact-line curvature alone brings about the qualitative difference in the evaporation mechanism. We rationalize it with the formalism of the modified Young's equation [Eq. (1)] as a result of the line tension [i.e., the additional term τ/R in Eq. (1)] τ/R on nanometer-sized spherical droplets. If we do this, we obtain negative values of the line tensions (below). Spherical, nanometer-sized droplets, thus, have smaller contact angles than larger droplets. The importance of the line tension was recently questioned by Ward and Wu [17]. These authors claimed that the solid-liquid interfacial tension is related to the fluid concentration (or pressure) in the solid-liquid interphase (adsorption). When taking this into account, they found that the dependence of the contact angle on the contact-line curvature can be completely accounted for by the adsorption instead of the line tension. In other words, the contact-line curvature leads to a modified effective solid-liquid interfacial tension, which varies upon adsorption, and no extra term depending explicitly on the contact-line curvature is required to complement Young's equation. This interpretation was challenged by Schimmele and Dietrich [18] who pointed out inconsistencies in the approach of Ward and Wu. In particular, according to these authors the role of pressure on the solid-liquid interfacial tension has been insufficiently addressed to draw definitive conclusions. Our interpretation of the difference in the evaporation mechanism cannot completely rule out the argument of Ward and Wu, as we have no information about pressure in the adsorbed liquid layers. However, the description of the liquid density oscillations near the surface, purportedly at the root of the modified γ_{sl} , can be extracted from our simulations. From the mass density profiles shown in Figs. S1, S2, and S3 in the Supplemental Material [19], it can be seen that the droplet shape (spherical versus cylindrical) has a very weak effect on the liquid structure near the interface (adsorption layers). The layer structure is present in each of the pairs C4 and S4, C6 and S6, and C7 and S7 with comparable intensities. The mass density distribution along the droplet main axis (Fig. S4 in the Supplemental Material [19]) delivers more precise information and shows marginal differences between each pair of two systems with the same surface attraction. Since the density distributions are very similar,

also the pressures in the adsorbed layers must be similar. Therefore, even a drastic change in the contact-line curvature does not have a strong effect on the liquid density profile. How a possible pressure difference affects the solid-liquid interfacial tension remains an open question.

It has also been argued that the modified Young's equation [Eq. (1)] is not valid at the nanometer scale due to the large curvature of the liquid-vapor interface and the curvature dependence of the associated interfacial tension in this curvature regime [5]. However, it has been shown that the liquid-vapor interfacial tension rapidly decreases with increasing droplet radius and converges to the value for the flat (zero curvature) interface when the radius reaches 10σ [6]. For droplets with larger radii like in our simulations, there is only a negligible difference in the interfacial tension between the planar and the curved liquid-vapor interfaces. Besides, Leroy and Müller-Plathe [22] have found that the contact angle of nanometer-sized droplets [radius down to $10\sigma(3.4 \text{ nm})$] could be predicted from the interfacial tensions of planar interfaces (i.e., for macroscopic droplets) while determining independently the liquid-vapor and solid-liquid interfacial tensions of Lennard-Jones systems. Therefore, it is justified to use Eq. (1) to derive the line tension approximately. We used the droplet geometry at various stages during the evaporation to probe the dependence of its contact angle on its radius. Although Young's equation describes the shape of a droplet at equilibrium, it was recently shown that the solid-liquid interface rapidly relaxes such that the interfacial tension should take its equilibrium value when the contact line moves during evaporation [25]. We assume that the droplet shape remains in quasiequilibrium as evaporation proceeds. We present in Fig. 3 the variations of $\gamma_{lv} \cos \theta_\infty - \gamma_{lv} \cos \theta_R$ with respect to $1/R$ for systems S4, S6, and S7.

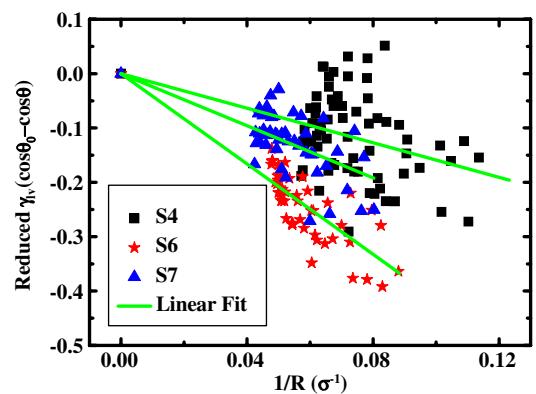


FIG. 3 (color online). Variation of $\gamma_{lv}(\cos \theta_\infty - \cos \theta)$ vs $1/R$ in reduced units for spherical drops with surface interactions $\varepsilon^* = 0.4, 0.6,$ and 0.7 for systems S4, S6, and S7, respectively. Only every third data point is shown in this profile for clarity. The green lines represent the results of fitting the modified Young's equation to the data, i.e., the lines are constrained to pass through the origin.

Applying a linear fit to each curve yields reduced values for τ (slope) which amount to $-1.6 \pm 0.1(-0.6 \times 10^{-11} \text{ N})$, $-4.1 \pm 0.1(-1.3 \times 10^{-11} \text{ N})$, and $-2.8 \pm 0.1(-0.9 \times 10^{-11} \text{ N})$ (the corresponding correlation coefficients are 0.83, 0.98, and 0.94) for $\epsilon^* = 0.4, 0.6$, and 0.7 , respectively. (Note that $\gamma_{lv}^* = 1.0(9.42 \text{ mN/m})$ [26] was used.) Despite the statistical uncertainty of these data, it is evident that the line tensions are all negative. This means [Eq. (1)] that the line tension lowers the contact angle of nanodroplets, i.e., it makes them flatter than they would be otherwise. It is also interesting to note that the values are all of the same order of magnitude and that they are in a good agreement with theoretical estimates and AFM experiments [3,8,13]. We cannot draw a firm conclusion about the influence of the solid-liquid interaction strength on the line tension due to the large uncertainties. Weijis *et al.* [8] found from equilibrium MD simulations at a much higher temperature that the magnitude of the line tension increases monotonically with the solid-liquid interaction strength. Our results are compatible with this trend, although there possibly is a minimum for system S6 in our case.

For values of the order of 10^{-11} N for liquid argon, it can be estimated that the line tension only starts to play a role for spherical droplets below $\sim 100 \text{ nm}$ in diameter. For these, the evaporation follows the observed mixed mechanism. Larger droplets (diameter $> 100 \text{ nm}$) evaporate from a heterogeneity-free surface at constant contact angle. If other evaporation mechanisms are found for large drops, they must be due to pinning at surface heterogeneities or impurities.

To summarize, by comparing the evaporation of spherical (with contact-line curvature) and cylindrical droplets (without contact-line curvature), we find that cylindrical droplets evaporate by decreasing their contact area at constant contact angle, whereas for spherical droplets both contact angle and contact area decrease simultaneously during evaporation. The role played by the curvature of the three-phase contact line can be explained using the concept of a line tension as a first-order correction to Young's equation. Its magnitude and sign are such that they significantly modify the contact angle of spherical nanometer-sized droplets during their evaporation. The calculated line tensions inferred for the Lennard-Jones systems studied here are negative and within an order of 10^{-11} N , if mapped to liquid argon, which is consistent with previous experimental and theoretical estimates.

This work is supported by the Collaborative Research Centre Transregio 75 Droplet Dynamics under Extreme Ambient Conditions of the Deutsche Forschungsgemeinschaft.

- *j.zhang@theo.chemie.tu-darmstadt.de
- [1] V. Raspal, K. O. Awitor, C. Massard, E. Feschet-Chassot, R. S. P. Bokalawela, and M. B. Johnson, *Langmuir* **28**, 11064 (2012).
 - [2] B. M. Law, *Phys. Rev. Lett.* **72**, 1698 (1994).
 - [3] J. K. Berg, C. M. Weber, and H. Riegler, *Phys. Rev. Lett.* **105**, 076103 (2010).
 - [4] A. Checco, P. Guenoun, and J. Daillant, *Phys. Rev. Lett.* **91**, 186101 (2003).
 - [5] Y. Liu, J. Wang, and X. Zhang, *Sci. Rep.* **3**, 2008 (2013).
 - [6] D. Zhou, F. Zhang, J. Mi, and C. Zhong, *AIChE J.* **59**, 4390 (2013).
 - [7] L. Guillemot, T. Biben, A. Galarneau, G. Vigier, and E. Charlaix, *Proc. Natl. Acad. Sci. U.S.A.* **109**, 19557 (2012).
 - [8] J. H. Weijis, A. Marchand, B. Andreotti, D. Lohse, and J. H. Snoeijer, *Phys. Fluids* **23**, 022001 (2011).
 - [9] L.-O. Heim and E. Bonaccorso, *Langmuir* **29**, 14147 (2013).
 - [10] J. Zhang, F. Leroy, and F. Müller-Plathe, *Langmuir* **29**, 9770 (2013).
 - [11] H. Y. Erbil, G. McHale, and M. I. Newton, *Langmuir* **18**, 2636 (2002).
 - [12] T. Furuta, M. Sakai, T. Isobe, and A. Nakajima, *Langmuir* **25**, 11998 (2009).
 - [13] D. Quéré, *Nat. Mater.* **3**, 79 (2004).
 - [14] T. Pompe and S. Herminghaus, *Phys. Rev. Lett.* **85**, 1930 (2000).
 - [15] J. Drelich, *Colloids Surf. A* **116**, 43 (1996).
 - [16] D. Winter, P. Virnau, and K. Binder, *Phys. Rev. Lett.* **103**, 225703 (2009).
 - [17] C. A. Ward and J. Wu, *Phys. Rev. Lett.* **100**, 256103 (2008).
 - [18] L. Schimmele and S. Dietrich, *Eur. Phys. J. E* **30**, 427 (2009).
 - [19] See Supplemental Material at <http://link.aps.org/supplemental/10.1103/PhysRevLett.113.046101>, which includes Refs. [20,21], for the interaction parameters, the simulation parameters, details about the calculation of contact angles and contact radii, and mass density distributions for the spherical and cylindrical droplets from additional equilibrium simulations.
 - [20] H. J. C. Berendsen, J. P. M. Postma, W. F. van Gunsteren, A. DiNola, and J. R. Haak, *J. Chem. Phys.* **81**, 3684 (1984).
 - [21] S. Plimpton, *J. Comput. Phys.* **117**, 1 (1995).
 - [22] F. Leroy and F. Müller-Plathe, *J. Chem. Phys.* **133**, 044110 (2010).
 - [23] J. H. Sikkenk, J. Indekeu, J. van Leeuwen, and E. Vossnack, *Phys. Rev. Lett.* **59**, 98 (1987).
 - [24] M. Schneemilch, N. Quirke, and J. R. Henderson, *J. Chem. Phys.* **118**, 816 (2003).
 - [25] A. V. Lukyanov and A. E. Likhtman, *Langmuir* **29**, 13996 (2013).
 - [26] D. Stansfield, *Proc. Phys. Soc. London* **72**, 854 (1958).